# Smart Antenna Gain versus Computational Load Increase Tradeoff Analysis on UMTS/TDD Uplink

D. Depierre[1], J. Thibault[1], G. Andrieux[2], JF Diouris[2]

[1] THALES Communications, Signal Processing Department
Multi Sensors Processing Laboratory
66, rue du Fossé Blanc
BP 156 – 92231 Gennevilliers Cedex (France)
e-mail : {david.depierre, joel.thibault }@fr.thalesgroup.com
[2] Ecole Polytechnique de l'Université de Nantes, IRCCyN
Rue C. Pauc
BP 50609 - 44306 Nantes Cedex 03 (France)
e-mail : {guillaume.andrieux, jean-francois.diouris}@polytech.univ-nantes.fr

**ABSTRACT**

Even if UMTS/FDD networks deployment encounters some delays, there is no doubt that UMTS/TDD will be implemented in a next future as its specific features (uplink/downlink asymmetry, low spreading factors) make it attractive to cover dense area where high bit rate services are required like railway station, exhibition rooms, conference halls, etc.
The result is that the study presented in this paper is focused on full load multi-user configurations (all code resources allocated to different users).
Despite a relative low number of simultaneously transmitting users (compared to FDD) allowing, on the uplink, powerful multi-users techniques, their performance remains insufficient to achieve targeted BER at full traffic load. Accordingly we addressed in this work comparative performance of two multi-user demodulation algorithms extended to the multi-sensor case (Array Joint Detection or AJD and Multistage Parallel Interference Cancellation or MPIC) in order to improve uplink capacity. In addition a complexity analysis is proposed bringing to light that MPIC algorithm offers the best performance/cost tradeoff.

## I. INTRODUCTION

Smart antenna as well as multi-user demodulation algorithms are well known powerful techniques able to improve cellular network transmissions capacity and/or quality of service. The point of the presented work is to bring, in the specific context of the reverse link of UMTS/TDD, quantitative results on array processing performance in realistic configurations either on simulated or real signals. Additionally, among all smart antenna benefits listed in [7], a system level evaluation address capacity improvement and coverage extension aspects in a simplified network context. Finally, previous results are weighted by a computational cost analysis of both tested demodulation algorithms.

*A .Tested Multi-user Algorithms*

The first multi-user/multi-sensor algorithm to be tested is the Array Joint Detection algorithm using Minimum Mean Square Error criterion (AJD-MMSE).
According to the multi-sensor received signal model :

$$\underline{e} = H\ \underline{d} + \underline{n}$$

where $\underline{d}$ stands for the multi-user transmitted symbols and $\underline{n}$ for the intercell interference plus noise component of the multi-sensor received signal, the AJD-MMSE estimates of users symbols are given by :

$$\hat{\underline{d}} = M\underline{e}$$

$M$ standing for :

$$M = \left(H^H R_n^{-1} H + R_d\right)^{-1} H^H R_n^{-1}$$

(for more details about AJD-MMSE algorithm refer to [2] and [3])

The studied alternative to AJD-MMSE is the well known Multistage Parallel Interference Cancellation (MPIC). The principle of this algorithm, as detailed in [5], is based on the same signal model. It is to apply-first a spatio-temporal matched filter whose expression is given hereafter :

$$\hat{\underline{d}}_{MF} = \sum_{k=1}^{K_a} H^{(k)H}\underline{e}^{(k)} = \underbrace{diag(R).\underline{d}}_{\textbf{Useful part}} + \underbrace{\overline{diag}(R).\underline{d}}_{\textbf{MAI+ISI}} + \underbrace{\sum_{k=1}^{K_a} H^{(k)H}\underline{n}_k}_{\textbf{Noise}}$$

with $R = \sum_{k=1}^{K_a} H^{(k)H} H^{(k)}$ ($H^{(k)}$ corresponds to the horizontal part of $H$ dedicated to the k[th] sensor).
As shown on the previous formula, as far as transmitted symbols are known, it is simple, at matched filter output, to isolate useful signal from MAI (Multiple Access Interference). As it is of course not the case, MPIC consists in an iterative process using the current estimated data symbols to refine data symbols estimate

for the next iteration. Using the estimated data symbols, estimated MAI contributions can be subtracted. The process is initialized using the array matched filter output as a first data symbols estimate.
This process applying direct MAI removal is given by :

$$\hat{\underline{d}}_{j+1} = \alpha_{j+1}\left(\hat{\underline{d}}_{MF} - \overline{diag}(R).Q\left(\hat{\underline{d}}_{j}\right)\right) + \left(1+\alpha_{j+1}\right)\hat{\underline{d}}_{j}$$

Where $\alpha_{j+1}$ is the current weighting factor in the iteration process. (For more details about optimal weighting factor design algorithm refer to [6])
It should be noted that both algorithms rely on a common channel estimation process specifically designed for UMTS/TDD waveform and where the different users channel IR are jointly estimated (cf. [4]).

*B. Evaluation Tool*

Algorithm performance evaluation was based on different means including as shown in Fig. 1, the following blocs : modulation, channel simulation or testbed measurements, multi-user combining plus noise addition and demodulation.

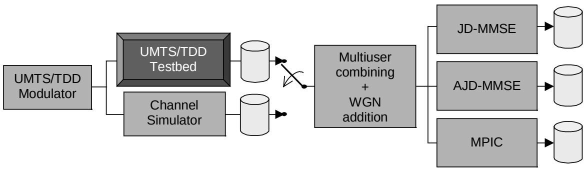


**Fig. 1. Simulation chain bloc diagram**

Channel simulator developed by France Telecom R&D comprises an antenna array transfer function simulation based on antenna arrays calibration measurements.
Another essential mean for algorithms evaluation is the real signal recordings database obtained from an uplink measurement campaign around THALES site in Gennevilliers. These signals were recorded using a testbed developed jointly by THALES, University of Nantes and FTR&D (the aforementioned simulation and testbed are described in more details in [1]).

## II. COMPARATIVE PERFORMANCE EVALUATION

The results presented in Fig. 2 and Fig. 3 were evaluated on simulated data using a spatial extension of the standard channel model "Vehicular A" with (Fig. 3) and without (Fig. 2) additional intercell interference.
The two multi-user configurations in Fig. 2 correspond to full load ones (all code resources are allocated). It appears clearly that as far as the channel IR is known, the influence of the number of users is negligible (except at high $E_b/N_0$ outside operational range). Logically, when channel IR is estimated, signal to noise ratio on the midamble part of the burst being inversely proportional to the spreading factor allocated to the user, results are worse for high spreading factors. The $E_b/N_0$ loss induced by noisy channel IR estimates, insignificant at SF 2, reaches 5 dB at SF 16. Finally AJD and MPIC shows similar results except for high $E_b/N_0$ where MPIC BER curve presents a floor unlike AJD, due to a non complete MAI removal. Increasing the number of iterations reduces the floor level but does not suppress it completely.

As illustrated in Fig. 3, the influence of intercell interference spatial distribution, perceptible for AJD algorithm when incident interference signal cone aperture decreases below 60°, is quite negligible on MPIC performance.

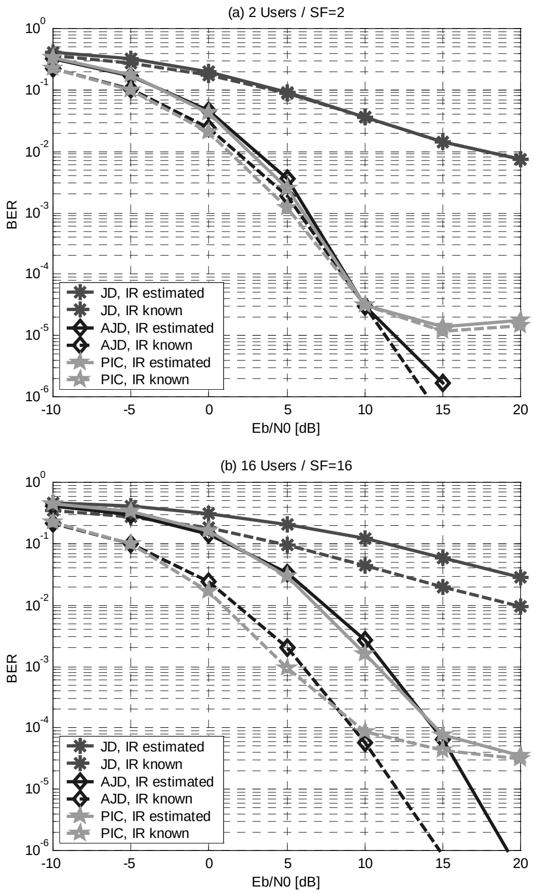


**Fig. 2. Algorithms performance with and without known channel on full load multi-user configurations**
**(a) 2 users at SF=2, (b) 16 users at SF=16**

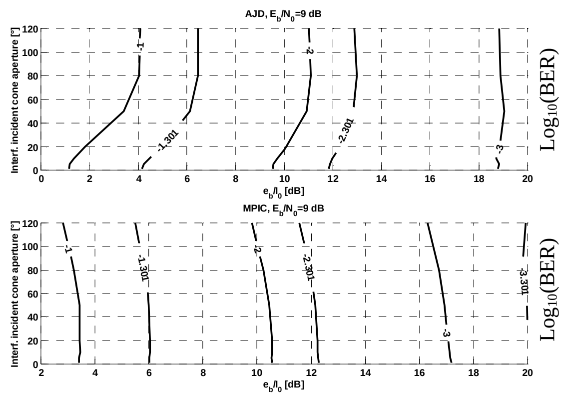


**Fig. 3. Intercell interference spatial distribution influence on array processing performance**
**(a) AJD, (b) MPIC**

At the opposite, Fig. 4 shows statistical results obtained with combinations of experimental single user signals (including extracell users with specific midamble and scrambling codes) recorded in outdoor environment.

The results which are synthesized in Fig. 4 correspond to five full load multi-user configurations with 6 extracell users uniformly spatially distributed in the 120° of the antenna azimuth coverage.

Each curve is the trace on ($E_b/N_0$, $E_b/I_0$) plane corresponding to the minimum ratios needed for a specific algorithm to deliver a target output BER of $5.10^{-2}$. As an example at a fixed $E_b/N_0$ of 8dB, relative $E_b/I_0$ gains of AJD (2 sensors) and AJD (4 sensors) versus JD (1 sensor) reach respectively 4.2 dB and 8.2 dB.

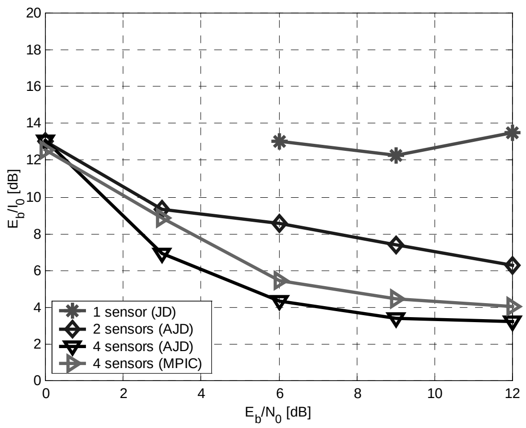


**Fig. 4. Statistical "iso-BER" (0.05) curves in ($E_b/N_0$, $E_b/I_0$) plane for OUTDOOR environment**

## III. CAPACITY AND RANGE EXTENSION GAINS

The evaluation of smart antenna influence in term of signal to interference and/or signal to noise ratios gains allows fruitful algorithms comparison. But to quantify the impact on network optimization these results have to be exploited in a system level analysis to evaluate how capacity and range extension are improved.

Similar approaches in [8] and [9] propose analysis of capacity enhancement brought by smart antenna for PCS and IS95 networks respectively. Both are based on theoretical single path propagation models.

The chosen approach for capacity gain evaluation is the following :

⇒ from link level results $E_b/I_0$ thresholds are extracted corresponding to the minimum energy per bit over interference power density needed to obtain a target BER (around $5\ 10^{-2}$),

⇒ simplified propagation and network models are applied to estimate *C/I* curves versus users density (number of user per cell) in the test cell (see Fig. 5).

⇒ from *C/I* curves and $E_b/I_0$ thresholds, variation in capacity gain with and without smart antenna are deduced as illustrated in Fig. 6.

Considering a simplified propagation model with an attenuation function of the distance given by :

$$Att(d) = \alpha\, d^4$$

and according to the network model described in Fig. 5, where only an averaged mobile position (center of the hexagon) is considered in each sector, the *C/I* curve versus the number of simultaneous users per cell at the base station has the following expression :

$$\left[\frac{C}{I}\right]_{UL}(n) = \frac{P \cdot r^{-4}}{\sum_i \left(n \cdot P \cdot d_i^{-4}\right)} = \frac{r^{-4}}{\sum_i \left(n \cdot d_i^{-4}\right)}$$

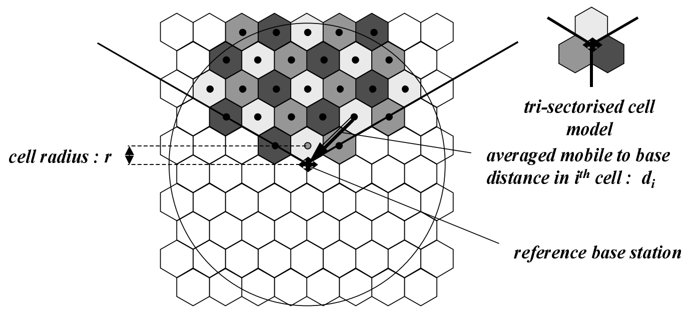


**Fig. 5. Intercell interference configuration for uplink in 120° sectorized network**

The intracell users are not taken into account in the interference component *I* as multi-user demodulation algorithms are considered.

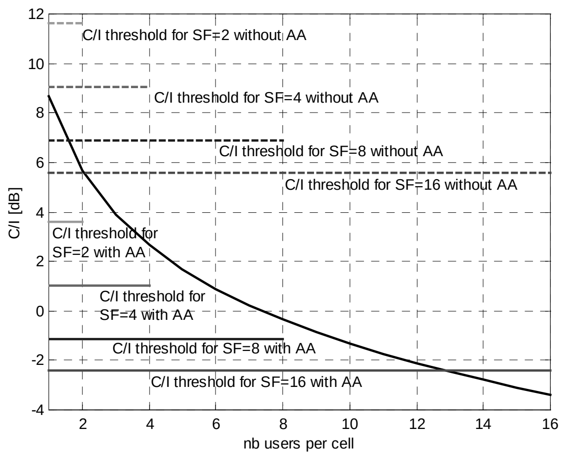


**Fig. 6. Uplink theoretical *C/I* curve versus cell load in an homogeneous 120° sectorized network**

As shown in Fig. 6, most working *C/I* threshold in the single sensor configuration are above the estimated *C/I* curve as those corresponding to the multi-sensor case are below. This implies that, in such uniform user distribution network with homogeneous service configuration, adaptive antenna is needed to overcome intercell interence and to allow full capacity transmissions.

This is summarised in Table 1 where the maximum number of users per cell reachable with and without smart antenna for the different spreading factor are mentioned.

| Spreading Factor | without AA | with AA |
|---|---|---|
| 2 | - | 2 |
| 4 | - | 4 |
| 8 | 1 | 8 |
| 16 | 2 | 12 |

**Table 1 : Maximum number of users per cell with an without Adaptive Antenna (on each uplink burst)**

The impact of adaptive antenna on range extension was evaluated in outdoor environment from $E_b/N_0$ gain obtained from outdoor measurements with the different antenna arrays. The cumulative probability density functions of the received signal strength (measured from outdoor measurements) are plotted in Fig. 7 for single sensor and multi-sensor antennas.

On this figure, the sensitivity gain appears in as the horizontal offset between multi-sensor curves and single sensor ones. As expected the median value at 50 % outage range is very close to the theoretical value of 6 dB for a four sensors antenna array.

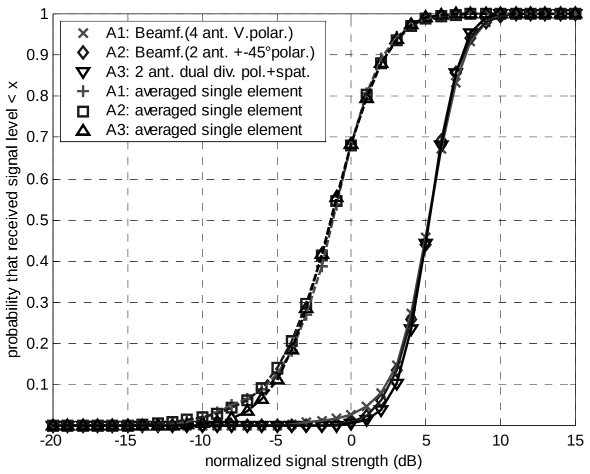


**Fig. 7. Characterisation of the sensitivity gain with respect to single sensor antenna**

Using the same propagation model as for *C/I* estimation, the coverage gain, expressed through the cell radius ratio with and without adaptive antenna, can be derived as follows :

$$Eb\_No\_SS - Eb\_No\_MS = Gain\_EbNodB = 10.\log\left(\frac{r_{SS}^{-4}}{r_{MS}^{-4}}\right)$$

$$\Rightarrow \frac{r_{MS}}{r_{SS}} = 10^{\frac{0.1}{4}.Gain\_EbNodB}$$

where *SS* stand for single-sensor and MS for multi-sensor.

It comes out that a gain of 6 dB in $E_b/N_0$ ratio allows to increase the cell radius by a factor of 1.4 corresponding to double the coverage area.

## IV. COMPLEXITY ANALYSIS

Even if the proposed smart antenna algorithms present attractive performance with respect to single sensor techniques, their use remains subject to the computational cost increase that they induce.

Consequently a detailed complexity analysis was led to compare both algorithms (AJD and MPIC), to identify the dimensioning parameters and to evaluate their influence on the total computational cost.

The results presented in Fig. 8 concern the number of elementary operations (here complex multiply-accumulate : MACC) needed to process one UMTS/TDD burst with the following default options :

- 5 users full load configuration
- channel length = 15 chips
- number of sensors = 4

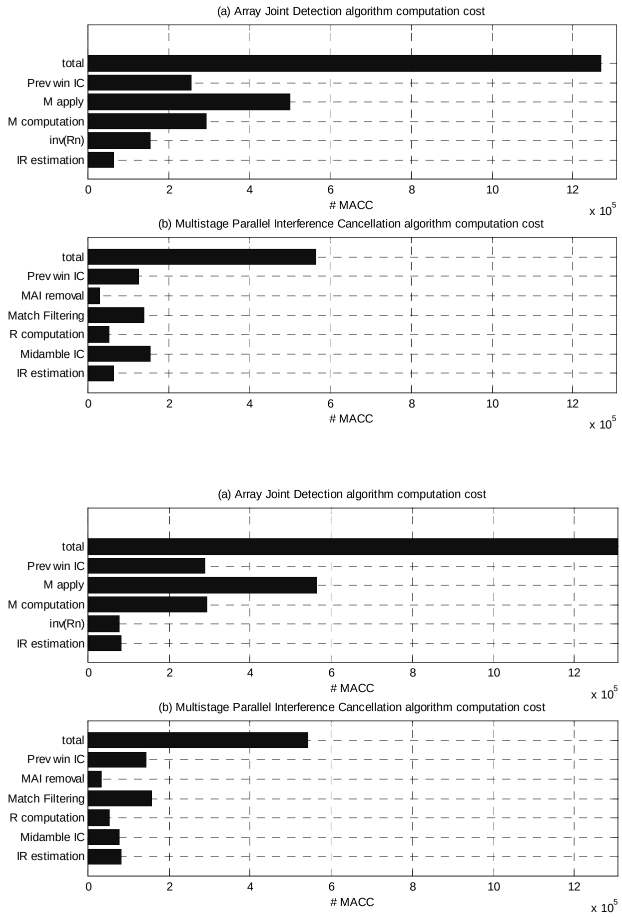


**Fig. 8. Computation cost evaluation in complex multiply-accumulate per UMTS/TDD burst, (a) type 1 / AJD, (b) type 1 / MPIC, (c) type 2 / AJD, (d) type 2 / MPIC**

Fig. 8 is split into upper part (a and b) and lower part (c and d) where the results are given for type 1 burst (midamble length of 512 chips) and type 2 burst (midamble length of 256 chips) respectively.

Within each part AJD and MPIC complexity are compared and detailed step by step.

From these results the following points come out:

- MPIC appears to be at least twice less complex than AJD,
- the influence of the burst type is not significant on complexity
- channel estimation is not the dimensioning step of the demodulation process

Computational cost depends on various parameters. Therefore, to assess more carefully algorithms complexity, cost variations versus main parameters (channel impulse response length, number of sensors and number of users) were investigated. The corresponding variation curves are presented in Fig. 9.

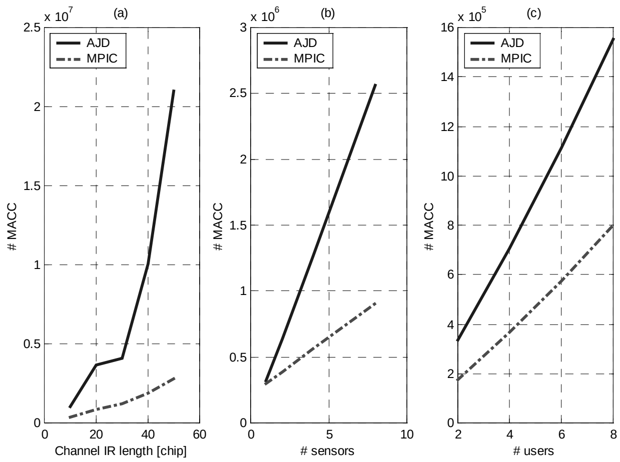


**Fig. 9. Computational cost parameters sensitivity**
**(a) Channel IR length,**
**(b) Number of sensors,**
**(c) Number of users**

Complexity variations are mostly linear except in Fig. 9 (a) where AJD complexity curve grows nearly exponentially versus channel IR length. In any case MPIC cost grows significantly slower than AJD one confirming that MPIC is by far the cheapest method to implement. Moreover MPIC does not require high dynamic floating point operation capabilities as AJD algorithm does to estimate inverse matrix.

To give an idea of the computational power needed to demodulate one uplink multi-sensor UMTS/TDD carrier, we fixed the number of uplink bursts per frame to 5 (one third) and we approximated AJD and MPIC computational costs to 13 $10^5$ MACC and 6 $10^5$ MACC respectively. The result is that, required computational power in scalar multiply-accumulate is given by the following expressions :

$P_{AJD} = 13\ 10^5 \times 5 \times 4 / 10\ 10^{-3}$ MAC/sec
$= 2.6$ GMAC/sec

$P_{MPIC} = 6\ 10^5 \times 5 \times 4 / 10\ 10^{-3}$ MAC/sec
$= 1.2$ GMAC/sec

As a matter of comparison, TI C67-167 and TI C62-300 realize 0.334 GMAC/sec (floating point) and 0.6 GMAC (fixed point) respectively.

## V. CONCLUSION

Two multi-user/multi-sensor demodulation techniques, AJD and MPIC, were evaluated either on simulated signals or on outdoor measured signals combinations.
Results showed very satisfactory performance for both algorithms. With four sensors, smart antenna reaches up to 8 dB versus single sensor demodulator on signal to interference ratio working threshold.
These link level evaluations translate into system level improvements in term of capacity an range extension increases.
However if both techniques perform similarly, computational costs present significant differences (MPIC is between 2 and 3 times less complex than AJD).
Finally, this work showed that as far as uplink is concerned, a smart antenna in conjunction with multi-user techniques constitutes a very attractive solution for demodulation stage in Rx process at the base-station, especially if the network is fully loaded. In this context MPIC algorithm seems to realize the best performance versus complexity tradeoff.

## REFERENCES


[1] J. Thibault, D. Depierre, “Smart Antenna for UMTS/TDD Uplink Improvement in Outdoor Environment”, IST Mobile Communications Summit 2001, pp 711-716

[2] P. Jung, J. Blantz, “Joint Detection with Coherent Receiver Antenna Diversity in CDMA Mobile Radio Systems”, IEEE Transactions on Vehicular Technology, Vol. 44, N°1, February 1995.

[3] C. Anton-Haro, X. Mestre and J.R. Fonollosa, “Array based and Joint Detection Method for the TDD Mode of UTRA”, PIMRC, Vol. 2, September 1999, pp. 253-257

[4] B. Steiner, P. Jung, “Optimum and Suboptimal Channel Estimation for the Uplink of CDMA Mobile Radio Systems with Joint Detection”, ETT, Special Issue on “Multiple Access in Radio Communication Networks”, Vol. 5, 1994,. pp. 39-50

[5] B. Steiner, “Interference Cancellation Vs. Joint Detection for the Uplink of the Joint Detection Mobile Radio Concept”, IEEE CDMA Techniques, May 1997

[6] D. Guo, L.K. Rassmussen, and T.J. Lim, “A Matrix Algebraic Approach to Linear Parallel Interference Cancellation in CDMA”, IEEE Trans. on Comm, Vol. 48, NO. 1, January 2000 pp. 152-161

[7] G.V. Tsoulos, “ Smart antennas for mobile communication systems: benefits and challenges ”, Electronics and Communication Engineering Journal, Vol. 11, NO. 2, April 1999, pp 84-94

[8] William C. Y. Lee, “Applying the Intelligent Cell Concept to PCS”, IEEE Transactions on Vehicular Technology, Vol. 43 NO.3, August 1994, pp. 672-679

[9] A.F. Naguib, A. Paulraj and T. Kailath, “Capacity Improvement with Base-station Antenna Arrays in Cellular CDMA”, IEEE Trans. on Vehicular Technology, Vol. 43 NO.3, August 1994, pp. 691-698